0026-895X/89/020265-08$02.00/0

MOLECULAR PHARMACOLOGY, 36:265-272

Multiple Opioid Receptors: Ligand Selectivity Profiles and Binding Site Signatures

AVRAM GOLDSTEIN and ASHA NAIDU

Department of Pharmacology, Stanford University, Stanford, California 94305

Received February 10, 1989; Accepted May 30, 1989

SUMMARY

Methods are described for studying μ, δ, and κ opioid binding sites, each without interference from the others. A large array of ligands has been characterized by ligand selectivity profiles, graphic depictions of affinities and selectivities. Binding site signatures have been derived, which uniquely describe each of the three types of sites. The μ, δ, and κ binding sites have interesting common features and distinctive differences.

To characterize multiple receptors, it is necessary to label one type or subtype[1] nearly exclusively. The history of binding studies with opioid receptors (2) illustrates this point. After receptor heterogeneity had been demonstrated (3), it was often mistakenly assumed that a ligand showing selectivity for one type of binding site would label that site without significant interference from other sites. For example, DADLE was assumed to label only δ sites, whereas the affinity of this ligand for μ is almost as great as for δ. Likewise, EKC, which elicited pharmacologic effects previously defined as being due to κ receptor activation, came into use as a radiolabel for κ binding sites even though its affinity for μ is almost as great as for κ.

Selective alkylation (4–6) was used in an attempt to enrich membranes with respect to one receptor type, but homogeneous populations could not be obtained. Sufficiently type-selective radioligands were required, and great progress has been made in several laboratories toward that goal. Sufficiently type selective means that the ratio of the affinity constant at the preferred (primary) site to that at the next-preferred (secondary) site is great enough so that binding at secondary sites is insignificant even when substantially more secondary than primary sites are present.

We report here the use of specific radioreceptor binding assays for opioid μ, δ, and κ sites to characterize each ligand by a LSP. LSP is the set of equilibrium dissociation constants for a given ligand at the three types of sites (7). The set of LSP data can be rearranged to yield a BSS for each site, a quantitative rank order of dissociation constants at that site. Each of the three sites studied here has a unique signature. We stress the conceptual difference between LSP, which characterizes a ligand, and BSS, which characterizes a binding site.

Experimental Procedures

Materials. Reagents were Baker analytical grade or equivalent unless stated otherwise. TB contains (mM): Tris-HCl, 50, pH 7.4. KHB contains (mM): NaCl, 118; KCl, 4.8; $CaCl_2$, 2.5; $MgCl_2$, 1.2; HEPES (Research Organics, Cleveland, OH), 25; pH adjusted to 7.4 with NaOH. KRB is the same as KHB with 1.2 mM KH_2PO_4 and 25 mM $NaHCO_3$ instead of HEPES and, in addition, 11 mM glucose and 0.02 mM choline chloride; mepyramine maleate (125 nM) was also present. KRB was bubbled constantly with 5% CO_2 in O_2 at 37° to maintain pH 7.4.

Peptides were from Peninsula Laboratories, unless otherwise stated, and were purified by reverse phase HPLC in our laboratory as required. For DYN A and DYN B and various fragments and derivatives of DYN A, see Ref. 8, and for DAKLI and its derivatives, see ref. 9. The following ligands are listed by code number; see also Figs. 3–5 and Table 2. **1**, OMF, Dr. Chi Zhiqiang (10); **2**, SUF (Janssen); **3**, DAKLI

This work was supported by Grants DA-1199 from the National Institute on Drug Abuse and BNS-84-16617 from the National Science Foundation.

[1] We call the μ, δ, and κ opioid receptors "types" after the terminology introduced by Ahlquist (1), who so described the α- and β-adrenergic receptors. Like α_1 and α_2, opioid receptor subtypes (if they exist) would have numerical subscripts.

ABBREVIATIONS: DADLE, [D-Ala^2,D-Leu^5]enkephalin; LSP, ligand selectivity profile; BSS, binding site signature; DAGO, [D-Ala^2,MePhe^4,Gly-ol^5]enkephalin; SUF, sufentanil citrate; OMF, ohmefentanyl hydrochloride, *N*-[1-(β-hydroxy-β-phenethyl)-3-methyl-4-piperidyl]-*N*-phenylpropionamide; DAKLI, dynorphin A analogue κ ligand; CTOP, cyclic D-Phe-Cys-Tyr-D-Trp-Orn-Thr-Pen-Thr amide; BREM, bremazocine hydrochloride; EKC, ethylketazocine methanesulfonate; β-NTA, β-naltrexamine; TB, Tris-HCl buffer; KHB, Krebs-HEPES buffer; KRB, Krebs Ringer buffer; HEPES, *N*-2-hydroxyethyl piperazine-*N*′-2-ethanesulfonic acid; DYN A-(1–13)-NH_2, dynorphin A-(1–13) amide; Me, methyl; Et, ethyl; Pr, propyl; DYN A, dynorphin A; DYN B, dynorphin B; HPLC, high pressure liquid chromatography; DSLET, [D-Ser^2,Leu^5]enkephalin-Thr; DPDPE, cyclic [D-penicillamine^2,D-penicillamine^5]enkephalin; SDL, specific displacement ligand; B_h-END, human β-endorphin; LEV, levorphanol tartrate; DEX, dextrorphan tartrate; β-NTA-I_2BH, diiodinated Bolton-Hunter reagent coupled to β-naltrexamine; β-NTA-F, fluorescein coupled to β-naltrexamine; DPLPE, [D-penicillamine^2,L-penicillamine^5]enkephalin.

(9); **4**, CTOP, Dr. V. J. Hruby (11); **5**, naltrexone hydrochloride (Endo); **6**, LEV (Roche); **7**, BREM (Sandoz) (12); **8**, DYN A-(1–13)-NH_2; **9**, β_h-END; **10**, oxymorphone hydrochloride (Endo); **11**, EKC (Sterling-Winthrop); **12**, DAGO (13, 14); **13**, biotinylated DAKLI, see Ref. 9 for preparation; **14**, [*N*-Me-Tyr^1]DYN A-(1–13)-NH_2; **15**, naloxone hydrochloride (Endo); **16**, diiodinated Bolton-Hunter reagent coupled to DAKLI, see Ref. 9 for preparation; **17**, β-NTA-I_2BH, see code **20** below; **18**, DADLE; **19**, morphine sulfate (Merck); **20**, β-NTA, National Institute on Drug Abuse; derivatives were prepared in our laboratory by standard coupling procedures and purified by reverse phase HPLC; **21**, DYN A (8); **22**, spiradoline (+)-enantiomer (U63,639) (Upjohn) (15); **23**, fluorescein coupled to DAKLI, prepared with fluorescein isothiocyanate and purified on reverse phase HPLC (9); **24**, [D-Abu^2,D-*t*-Leu^5]enkephalin (16); **25**, DSLET, Dr. B. P. Roques (17); **26**, DYN A-(1–13); **27**, spiradoline (−)-enantiomer [U63,640] (Upjohn) (15); **28**, β-NTA-F, see code **20** above; **29**, DPLPE(Me) (16); **30**, morphiceptin (18); **31**, DPDPE(Me) (16); **32**, DPLPE(Et) (16); **33**, DPDPE(Me)$_2$ (16); **34**, DPLPE (16); **35**, DYN B (8); **36**, (*trans*)-3,4-dichloro-*N*-methyl-*N*-[2-(1-pyrrolidinyl)cyclohexyl]benzeneacetamide methanesulfonate (U50,488) (Upjohn) (19); **37**, DYN A-(1–9); **38**, DEX (Roche); **39**, DPDPE, Dr. H. I. Mosberg (20); **40**, DYN A-(1–6); **41**, DPLPE(Pr) (16); **42**, DPDPE(Et) (16); **43**, DPDPE(Pr) (16); **44**, DYN A-(1–7); **45**, [D-*t*-Leu^2,D-*t*-Leu^5]enkephalin (16); **46**, D-(5α,7α,8β)-(+)-*N*-methyl-*N*-[7-(1-pyrrolidinyl)-1-oxaspiro-(4,5)dec-8-yl]benzeneacetamide (U69,593) (Upjohn) (21); **47**, DYN A-(1–8).

Membranes. A guinea pig was decapitated and the whole brain (in some experiments, less cerebellum) was weighed (about 3 g) and frozen immediately on dry ice. Brains could be stored for several months at −70° without loss of binding capacity. The tissue was homogenized (Tekmar Tissumizer, Cincinnati, OH) in 30 ml of KRB at 37°. After centrifugation (12,000 × *g*, 23°, 10 min), the pellet was resuspended in KRB to about 90 ml and incubated (37°, 20 min) in tightly capped tubes to destroy endogenous opioids. After another centrifugation, the membranes were resuspended to about 180 ml, subdivided into three portions with each made up to 200 ml, capped again, and incubated as above. There followed two rounds of centrifugation (16,000 × *g*, 23°, 10 min) and resuspension in the same volume of KHB or TB (whichever was to be used in the binding assay). The membrane pellet was dispersed with a Dounce B homogenizer, at 23°, to make a homogeneous suspension (typically 150 ml) of which each milliliter represents 20 mg of original brain and has about 0.2 mg of protein.

Radioreceptor binding assay. Each radioligand was used at the lowest practical concentration, to provide about 1500–3000 cpm of site-specific binding. SDL signifies a specific-displacement competing ligand, to define specific binding by difference. Each SDL concentration was chosen because it produced a plateau in the competition curve or was at least 10 times the K_d of the given radioligand. Conditions for the μ system were [^{3}H]DAGO (48 Ci/mmol; NEN, Boston, MA) 0.8 nM in TB and 2.0 nM in KHB, with 300 nM DAGO as SDL; for the δ system, [^{3}H]DPDPE (28 Ci/mmol; Amersham, Chicago, IL) 1.0 nM in TB and 2.0 nM in KHB, with 100 nM DPDPE as SDL. Specific binding was 83 and 70% of total binding for [^{3}H]DAGO and [^{3}H]DPDPE, respectively.

For labeling κ sites, no sufficiently selective radioligand was available, so a "paired-tube" paradigm was devised. [^{3}H]BREM (30 Ci/mmol; NEN) is a high affinity radioligand with modest selectivity for κ sites, whereas U50,488 (not available as a radioligand) is highly selective for κ sites. Specific κ binding was, therefore, defined as the difference between the binding of 75 pM [^{3}H]BREM in the absence and presence of 500 nM U50,488 in matched pairs of tubes at every concentration of a competing ligand. In some of these experiments, 5 nM DAGO and 50 nM DPDPE were present to block μ and δ sites, but the paired-tube differences proved to be virtually the same with and without the blockers. When [^{3}H]BREM binding was plotted against log concentration of U50,488, the residual binding at the plateau (i.e., to other than κ sites) was about 35% of total binding.

Components were added in the following order to a polypropylene test tube: buffer, 0.5 ml, containing SDL and blockers as required, or buffer alone; membrane suspension, 1.0 ml kept agitated by swirling; 10 μl of methanol/0.1 M HCl (1:1, v/v) containing competing ligand or methanol/HCl alone; and radioligand in buffer, 0.5 ml. Incubation (23°, 2 hr) was demonstrated, with each radioligand and competing ligand, to be long enough for equilibration. Samples were kept on ice (less than 15 min) until filtration (S&S No. 32 glass fiber filters, 24 mm, presoaked in glass-distilled water that was saturated with *t*-amyl alcohol) in an aluminum filter block. Alternatively, No. 32 glass fiber strips were prepared in the same way and used in a cell harvester (M24R; Brandel, Gaithersburg, MD). Tubes were washed onto the filters three times with 4 ml of cold buffer. Filters were transferred to scintillation vials and allowed to stand at room temperature in 5 ml of Cytoscint (Westchem, San Diego, CA) for at least 5 hr, the time required to dissolve all radioligands and attain maximum cpm. Radioactivity was counted to 1.5% SD or for 100 min.

Radioligand dissociation constants (K_d) were determined in TB and KHB from binding isotherms with the LIGAND program (22). Best fits for the δ and κ systems were obtained with a one-site model, but [^{3}H]DAGO binding was fitted best by a two-site model (Fig. 1). As elaborated upon in the Discussion, we used the high affinity estimate of DAGO K_d in computations of K_i for competing ligands. Data are summarized in Table 1. K_d values differed less than 2-fold in the two buffers. B_{max} varied widely at different times and among brains; isotherms in KHB and TB were usually not carried out concurrently and, inasmuch as B_{max} differences as large as severalfold were also observed in different experiments with the same buffer, we cannot attribute the differences observed here to the buffers.

To avoid errors due to unrecognized depletion (23), free radioligand concentrations were measured routinely by determining radioactivity in supernatants from parallel sets of tubes, which were centrifuged instead of filtered after the incubation, and interpolating to the IC_{50} (concentration at which specific binding is reduced by half). The percentage of depletion by binding in the absence of a competing ligand was only 6% (SE, 2%) for [^{3}H]DAGO (3 experiments) and 8% (SE, 2%) for [^{3}H]DPDPE (11 experiments) but 43% (SE, 1%) for [^{3}H]BREM (17 experiments). A full equation (23) was used instead of the Cheng-Prusoff approximation (24) to convert IC_{50} to K_i for each competing ligand:

$$K_i = \{1/[(2L/L_0) + (L/K_d) - 1]\}\ IC_{50}$$

where the measured free radioligand concentrations are L_0 in the absence of a competing ligand and L at the IC_{50}. In over 100 experiments conducted over a period of many months (23), IC_{50} (and therefore K_i) was determined with a SD of 0.1 decimal log units (i.e., about 25%).

Because it is impractical to measure free concentrations of high affinity unlabeled competing ligands, whenever an observed IC_{50} is less than the radioligand K_d the computed value of K_i may be too large by an indeterminate amount (23).

Radioligands and competing ligands were checked for purity by reverse phase HPLC (Waters Associates C_{18} μBondaPak column, 3.9 × 30 cm, 30-min linear gradient of acetonitrile in 5 mM trifluoroacetic acid with gradients optimized for each ligand) and were purified by HPLC as necessary. The integrity of the three radioligands after the 2-hr contact with membranes was examined by the same method; no degradation was observed. Peptide competing ligands (e.g., dynorphin peptides), at low concentrations, are known to be degraded to a variable extent, and no suitable protective "cocktails" could be devised. Some such ligands are protected while occupying a binding site (9) but we do not know how general this phenomenon is; therefore, some peptide competing ligands may have higher affinities than we estimate.

Results

If more than than a few percent of radioligand is bound to secondary sites, especially if secondary sites outnumber primary sites, erroneous K_i values will be computed for competing

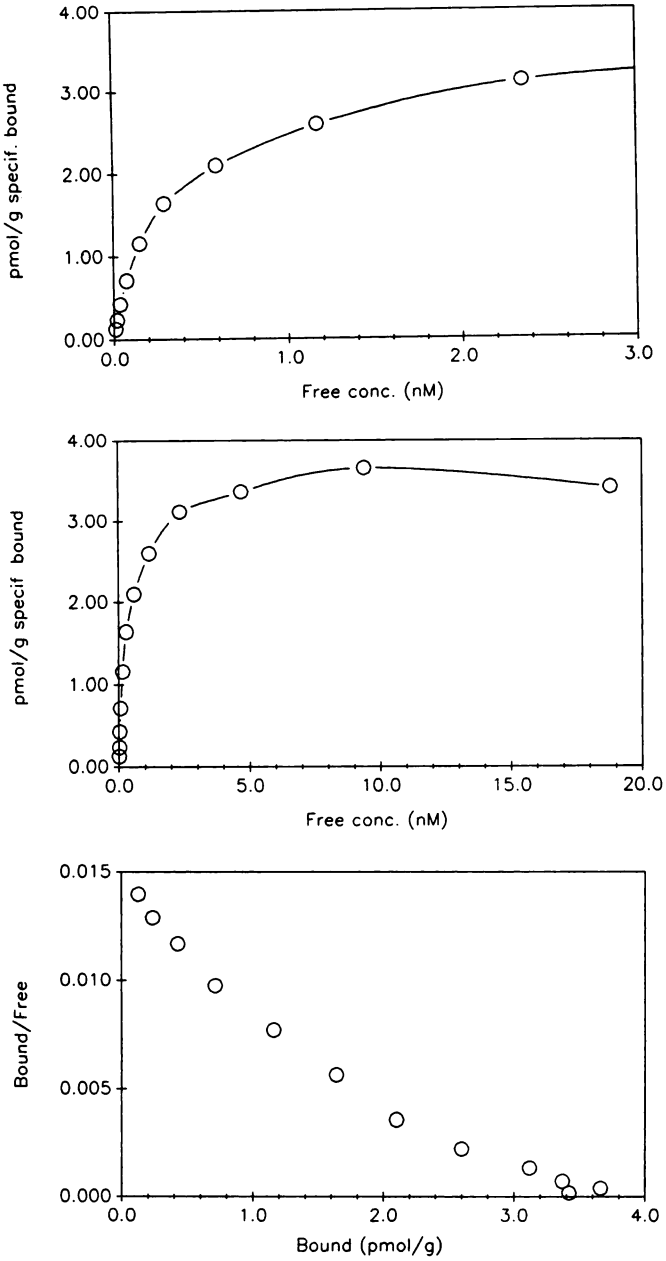

Fig. 1. [^{3}H]DAGO binding. *Top* and *middle*, Saturation binding isotherms; note wide range of concentrations tested and different *x*-axis scales. *Bottom*, Scatchard transformation of all the data. A typical experiment in TB is shown; data from several experiments are summarized in Table 1.

TABLE 1

Binding isotherm results in the μ, δ, and κ systems

For details see Experimental Procedures. *n* denotes independent experiments performed on different days and with different brains. B_{max} is expressed in terms of original wet weight of brain tissue. Data have been rounded to two significant figures.

^{3}H-labeled radioligand	Buffer	*n*	K_d	SE	B_{max}	SE
			nM		*pmol/g*	
DAGO						
High affinity	TB	3	0.14	0.01	1.6	0.2
	KHB	3	0.24	0.04	0.82	0.10
Low affinity	TB	3	1.3	0.1	2.0	0.2
	KHB[a]	3	270.	74.	12.	5.
DPDPE	TB	7	2.0	0.1	5.0	0.3
	KHB	3	1.5	0.1	1.1	0.1
BREM	TB	6	0.020	0.002	3.9	0.4
	KHB	3	0.020	0.003	2.8	0.4

[a] Note uncertainty of this estimate, based on multiple points near saturation.

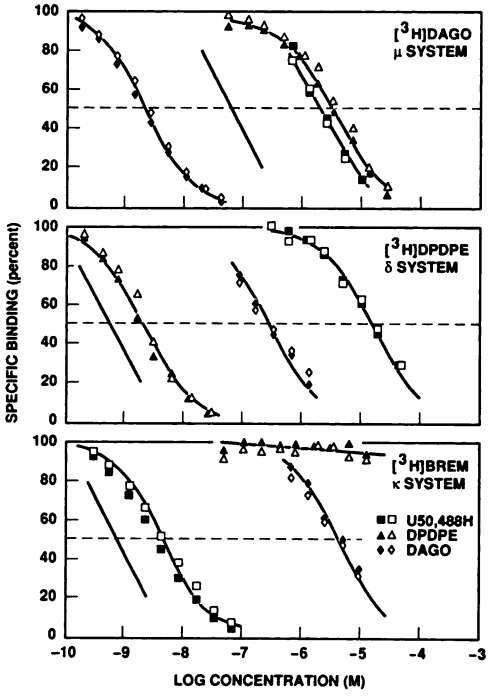

Fig. 2. Homologous and heterologous competition curves in the μ, δ, and κ systems. The buffer was TB. See Experimental Procedures for details of the assays. *Open* and *filled symbols* on each graph represent independent experiments carried out at least 1 month apart. *Straight lines* are log-logit slopes of unity, corresponding to simple mass-law interaction.

ligands. A linear Scatchard plot is no proof of site homogeneity; two sites present in equal numbers and differing by 5-fold in K_d yield a straight line with linear regression coefficient >0.99. Nor is a smooth, symmetrical, self-competition curve with log-logit slope of unity any better proof; self-competition is very insensitive to site heterogeneity.

The most conclusive way to prove that a radioligand labels a single homogeneous site population is to demonstrate that ligands that are highly selective for nonpreferred (secondary) sites yield smooth competition curves with appropriate slopes. If an appreciable fraction of a radioligand is bound at a secondary site, even though the self-competition curve is smooth, a competing ligand that is selective for the secondary site will produce an irregular curve. At low concentrations it will reduce binding by some small amount, to produce a distinct plateau, followed by reduction of the remaining bound radioligand at higher concentrations. Absence of such early plateaus in heterologous competition curves indicates adequate selectivity of a radioligand.

Fig. 2 shows typical smooth competition curves obtained in TB at the three sites labeled as described in Experimental Procedures. Similar results were obtained in KHB (not shown). Here we have depicted, for each radioligand, both the self-competition curve and the heterologous competition curves with ligands the affinities of which are orders of magnitude greater for their own preferred sites than for the labeled primary site.

From log-logit transformations of such curves, we found IC_{50}

values by linear regression analysis, and we computed K_i values as described. Selectivity is described by the ratio of the dissociation constant at each secondary site to that at the primary site. Because concentration increments in a competition curve are geometric, selectivity is best displayed in a LSP (7) as a linear difference on a logarithmic scale of K_i values.

Figs. 3–5 show LSPs for 33 ligands, the affinities and selectivities of which are evident at a glance. Code numbers reflect the order of decreasing affinity for the μ site. The site selectivity of the three key ligands (DAGO, Code **12**; DPDPE, Code **39**; and U50,488, Code **36**) can be assessed by inspection of the topmost LSP in Figs. 3A, 4, and 5B, respectively; each affinity for a primary site is more than 2 orders of magnitude greater than that for the next-preferred secondary site.

LSP was determined in TB without added salts and in KHB that contained salts at physiologic concentrations. The well known effect of salts on K_i (25–27) is seen here as about an average 2-fold increase but is sometimes negligible or absent and is occasionally very large. Especially interesting is the large shift with CTOP, in view of the fact that this compound is a μ receptor antagonist (28); it would be interesting to study the effect of sodium alone on CTOP in this regard, to test whether the sodium shift necessarily distinguishes generically between agonists and antagonists (25, 26). Also interesting is the effect of salts on DYN A-(1–9), changing its selectivity from κ to μ.

Fig. 3 shows LSPs for several μ-selective ligands. The relatively poor selectivity of morphine for μ sites is evident here, as compared with DAGO, SUF, and OMF. It is noteworthy that, in this series, higher selectivity appears to be primarily due to increased affinity at μ, without much change in affinity for δ or κ. OMF is a novel fentanyl derivative (10); it could be superior to [^{3}H]DAGO as a μ-selective radioligand and its high affinity and selectivity, as compared with morphine, might well make it a superior analgesic agent. The higher μ selectivity of morphiceptin than of morphine shows that selectivity and affinity can vary independently. β_h-END is clearly selective for μ over δ and κ. The comparison of LEV and DEX shows that the stereoselective preference for the (−)- over the (+)-enantiomer, to the extent of several orders of magnitude, applies to about the same degree to all three types of binding sites. The results with DEX are not due to traces of LEV (unpublished data).

Substitution on the 6-position of naltrexone has interesting effects (Fig. 3B). Conversion of keto to amino (in β-NTA) causes a dramatic loss of μ and δ affinity without much change in κ affinity. Coupling iodinated Bolton-Hunter reagent to β-NTA (β-NTA-I_2 BH) causes a selective loss of κ affinity. Finally, coupling with fluorescein (β-NTA-F) causes differential changes of affinity that result in a δ-selective ligand.

In Fig. 4, we show LSPs for three δ ligands; data for many others, published elsewhere (16), are not repeated here. The LSP of DADLE shows very clearly that this compound, although technically δ selective, barely distinguishes δ from μ. DSLET is a modest improvement, but it is the cyclic structure of DPDPE that evidently stabilizes an optimal conformation for δ sites.

Fig. 5A is consistent with our previous findings (29, 30) on how the κ selectivity of DYN A depends primarily on residues 11 and 13. DYN A-(1–9) is κ-selective only in TB, and smaller fragments are actually μ selective. DYN B, as previously reported (29), is κ selective.

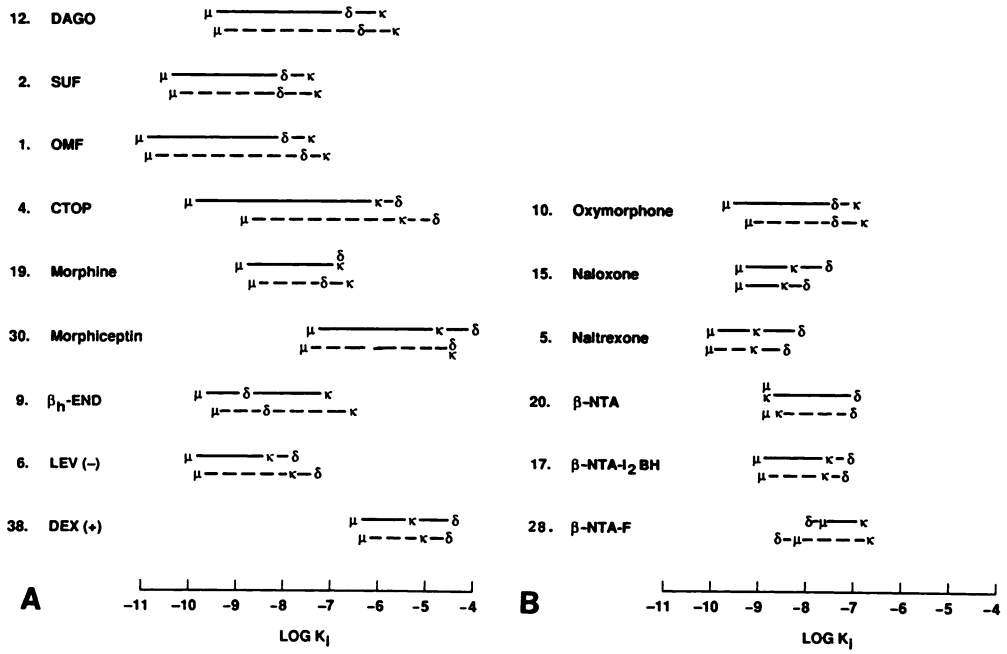

Fig. 3. Ligand selectivity profiles of μ-selective ligands. For each ligand, the logarithms of the dissociation constants, K_i, were computed from log (IC_{50}) values by linear regression analysis of a log-logit transformation of the competition curves. Greek letters, μ, δ, and κ, are positioned at log (K_i) for each binding site, with highest affinities at the *left*. Assays were carried out in TB without mineral salts (*upper of pair*, *solid line*) and in KHB containing salts at physiologic concentrations (*lower of pair*, *broken line*). *Data points* are means of the values from at least two or three independent competition experiments. The SD of such independent estimates of IC_{50} in our hands was 0.1 log units. In each experiment, the competition curve was generated by concentration doublings of the competing ligand, with triplicate incubation tubes at each concentration. Ligand selectivity is represented here by the horizontal distance between the preferred (highest affinity) site and the next-preferred site. See Experimental Procedures for details of the assay systems. This legend applies also to Figs. 4 and 5. Numerical codes correspond to the order of affinities for μ sites; these same code numbers are used to represent the ligands in Table 2.

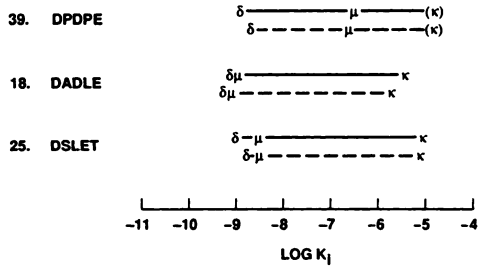

Fig. 4. Ligand selectivity profiles of δ-selective ligands. For additional δ-selective ligands, see Ref. 16. See also Fig. 3 legend.

Fig. 5B presents the LSP of the highly κ-selective U50,488 and U69,593 and of BREM and EKC, which have higher affinity but poorer selectivity for κ sites. The enantiomers U63,640 and U63,639 are extremely interesting; here, a high affinity, highly selective, κ ligand becomes a high affinity, highly selective, μ ligand by virtue of a 10,000-fold loss of κ affinity without major change in μ or δ affinity.

The quantitative rank order of affinities of a set of ligands at a binding site uniquely defines that type of site by a BSS. Table 2 presents the BSS patterns of the three sites under study here. Each includes the set of $-\log(K_i)$ values for 47 ligands that are designated by numerical codes as in Experimental Procedures.

There is a consensus rank order of affinities among the three sites, disrupted by a few ligands that have low affinity for one site but very high affinity for another. The "consensus breakers" that distinguish the δ sites are the cyclic enkephalin analogues DPLPE (Code **34**) and DPDPE (Code **39**) and a few of their derivatives, which have very poor affinities for μ and κ but catapult more than 2 orders of magnitude to the top of the δ BSS. Similarly, U50,488 and U69,593 are at the bottom of the list at both μ and δ sites but have greater affinity by 3 orders of magnitude at κ sites.

Fig. 6 presents correlation plots for affinities at pairs of sites. When each $\log(K_i)$ value at δ is plotted against $\log(K_i)$ at μ (Fig. 6A), the correlation coefficient is 0.47 ($p < 0.01$). For κ against δ (Fig. 6B), the corresponding statistic is 0.19 ($p > 0.05$), and, for μ against κ (Fig. 6C), it is 0.54 ($p < 0.01$). Thus, the δ signature differs from κ more than from μ and more than μ and κ differ from each other.

Discussion

The graphic LSP offers the following advantages. (a) Dissociation constants are compared, not IC_{50} values, which vary according to affinities and concentrations of the particular radioligands used. (b) The essential information makes an instantaneous and readily interpretable visual impact. (c) The logarithmic scale means that, as is appropriate for comparisons of selectivity, the same horizontal distance represents the same ratio of dissociation constants, regardless of the absolute affinities. (d) The smallest horizontal distance that is discernible (about 0.1 decimal log units) corresponds roughly to the experimental error (approximately 25%) in determining the IC_{50} values from which dissociation constants are derived (23). (e) In comparing ligands that differ in selectivity for a given site, the two possible causes, difference in affinity for the preferred site and difference in affinity for the next-preferred site, are instantly distinguished by eye.

Concerning LSPs, we have provided quantitative confirmation that certain ligands meet the requirement of sufficient selectivity, namely, that there be at least 2 or 3 orders of magnitude difference in affinity for the preferred site relative to the next-preferred site. DAGO is acceptable for μ sites but ohmefentanyl is better, and CTOP is better yet. DPDPE and DPLPE are acceptable for δ sites. U50,488 and U69,453 are suitable at κ sites; the latter is not significantly more selective, but, unlike U50,488, it is now available as a ^{3}H-labeled radioligand.

As noted in Experimental Procedures, there is uncertainty about the [^{3}H]DAGO K_d. Our high affinity estimate is derived from very low concentrations. We began with the lowest concentration that yielded measurable binding (9 pM), with con-

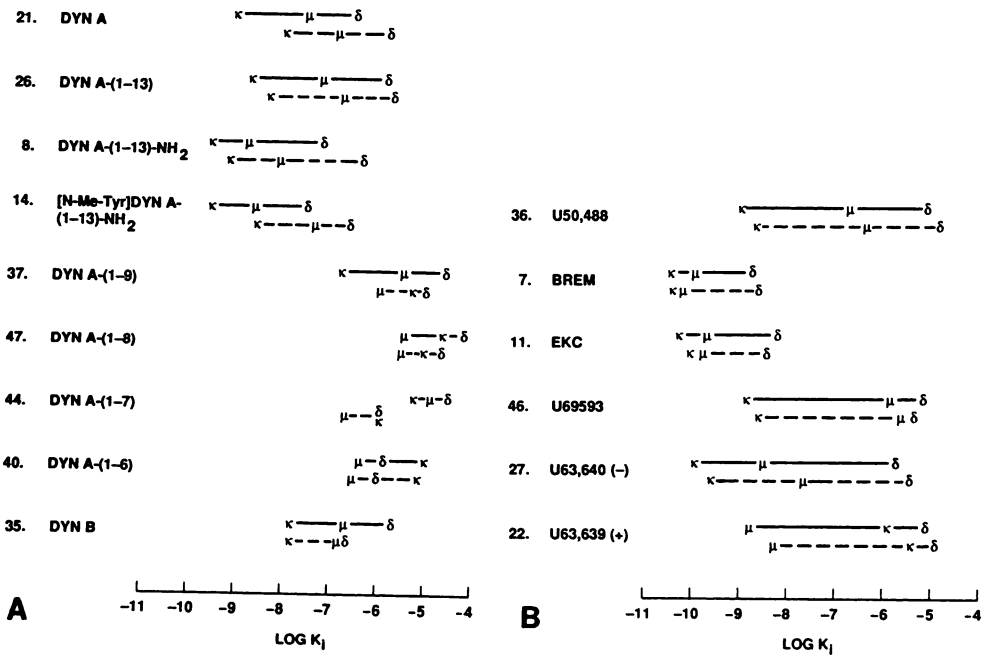

Fig. 5. Ligand selectivity profiles of κ-selective ligands. For additional κ-selective ligands, see Ref. 9. See also Fig. 3 legend.

TABLE 2

Binding Site Signatures

The same ligands depicted in Figs. 3–5 and others from Refs. 9 and 16 are arranged here vertically, by numerical code, according to $-\log(K_i)$ in TB at the three types of binding sites, with highest affinity at the top. Numerical codes and other information about the ligands in Experimental Procedures. Parentheses indicate that the true value of K_i was greater, $-\log(K_i)$ numerically smaller, than could be measured. For structures and binding data of derivatives of the cyclic enkephalin analogues DPDPE and DPLPE, see Ref. 16. For structures and binding data for the DYN A analogue DAKLI series, see Ref. 9.

$-\log(K_i)$	μ	δ	κ
11.1	1		
11.0			
10.9			
10.8			
10.7			3, 8
10.6	2		13, 14
10.5			
10.4			7, 16
10.3			11
10.2			21
10.1	3		
10.0	4, 5, 6, 7		27
9.9	8		26
9.8			
9.7	9, 10, 11		
9.6	12, 13		23
9.5	14		
9.4	15, 16		
9.3			
9.2		34	
9.1		18	
9.0	17, 18	25	5, 36
8.9	19	39	46
8.8	20	7, 9	20
8.7	21, 22	3	
8.6	23, 24		
8.5	25, 26, 27	14	
8.4		8, 29	
8.3		11	
8.2		16	6, 15
8.1		5, 13, 23	
8.0		1, 2, 28	
7.9			35
7.8		6, 21, 24	
7.7			
7.6	28, 29	41	
7.5		15, 42	1, 2, 17
7.4	30	10	
7.3		31, 32	
7.2	31	33	
7.1		17, 26	9
7.0	32		10, 37
6.9		19, 20, 43	19
6.8	33, 34		28
6.7	35, 36		
6.6	37	12	
6.5	38, 39		47
6.4	40, 41		
6.3	42, 43	45	
6.2			44
6.1			
6.0	44, 45		12
5.9	46	40	22
5.8	47	27, 35, 37, 44	4
5.7			
5.6		4	
5.5			
5.4		47	18
5.3		46	38
5.2		22	
5.1		36	(25), 40
5.0			
4.9			45
4.8			(39)
4.7			24, 30, 33
4.6		(38), (30)	29, 31, 32, (34), 41, 42, 43

centration doublings spanning a very large range (to 19 nM). Most data in the literature (e.g. Refs. 14 and 31) cover only the upper range and consequently reflect only the low affinity site, with K_d approximately 1 nM. For competition curves, we used 0.8 nM [^{3}H]DAGO, 5.7 times the K_d of the high affinity site but only 0.62 times the K_d of the low affinity site. For the relative site densities given in Table 1, computation shows that 64% of the label is in high affinity sites, the properties of which should chiefly govern the competition results. If conversions of IC_{50} to K_i were based on the low affinity K_d, all $-\log(K_i)$ values at μ sites in Figs. 3–5 would be moved 0.97 log units to the right and in Table 2 all entries under the μ column would move down by the same amount.

It may be that the high affinity [^{3}H]DAGO site represents a high affinity state rather than a distinct subtype and that it predominates in our membrane preparation because of removal of regulatory guanyl nucleotides (32) during the extensive washing and preincubation steps. The possibility that it corresponds to μ_1 (33) is not suggested by our data, but it cannot be rigorously excluded; however, under our conditions the site(s) labeled by [^{3}H]DAGO show(s) classical μ behavior, as evidenced by all the profiles in Figs. 3–5.

The set of truncated and otherwise modified DYN A derivatives is of interest in confirming results of pharmacologic assays (5, 29, 30), showing that κ selectivity seen in DYN A, DYN A-(1–13), and DYN A-(1–13)-NH_2 is progressively lost on C terminal truncation beyond lysine-11. The critical role of lysine-11 is consistent with the effectiveness of a novel selective ligand, [D-Pro^{10}]DYN A-(1–11) (34), but shorter fragments such as DYN A-(1–8), which have also been proposed, are not suitable. It is interesting that the fragment 1–6, i.e., [Leu]enkephalin-Arg^6, is μ selective, whereas [Leu]enkephalin itself is δ selective.

LEV (Code **6**) and DEX (Code **38**) demonstrate that essentially the same degree of stereoselectivity applies at all three sites, i.e., the LSPs are virtually the same except for the absolute affinities. However, a quite different pattern is seen with U63,640 (−) (Code **27**) and U63,639 (+) (Code **22**); the affinities are not greatly different at μ and δ, but the affinity of the (−)-enantiomer at κ is more than 10,000 times that of the (+)-enantiomer.

BSSs shed light on the similarities and differences among the opioid binding sites. The multiple opioid receptors all recognize naloxone and naltrexone as antagonists in biologic assays; indeed, such blockade is the *sine qua non* for defining a receptor as opioid. With antagonists, potencies in bioassays should be directly reflective of binding affinities. Accordingly, in Fig. 3B, naloxone shows a preference of about 10-fold for μ over κ and greater preference for μ over δ, as in bioassays (3). All the opioid receptors require that a ligand have a basic amino group (in peptides usually the α-amino group of N terminal tyrosine) at a certain distance from a phenolic or other aromatic ring. Another common requirement is for a T conformation produced by two hydrophobic rings at a certain angle to each other. Finally, all the opioid receptors display very strong stereoselectivity in their interactions with ligands. Thus, it is not surprising that there is a consensus quantitative rank order of ligand affinities across the μ, δ, and κ binding sites. It is the consensus breakers that uniquely distinguish each site. No opioid receptor has yet been cloned, so the molecular basis of the differences, different genes, differential splicing, or post-translational modification, is unknown.

Claims have been advanced for the existence of novel opioid

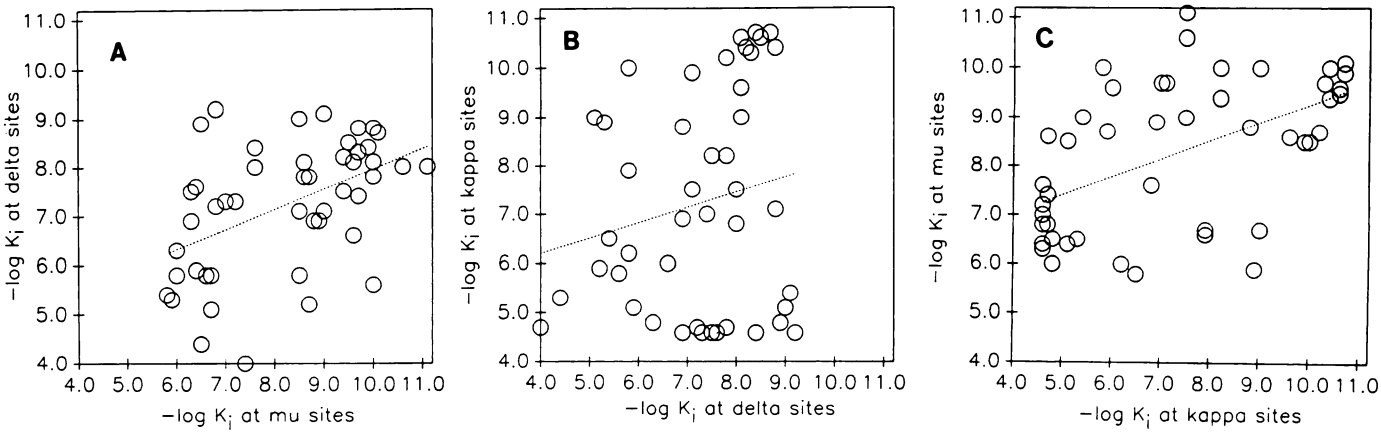

Fig. 6. Correlation plots for 47 ligands at pairs of sites. Each *point* represents −log(K_i) at a site on the *y*-axis and another site on the *x*-axis. Here highest affinities are to the *right* and *top* of each plot. Least squares regression lines are shown; see text for correlation coefficients. A, δ versus μ; B, κ versus δ; C, μ versus κ.

receptor subtypes. Until cloning and sequence analysis provide conclusive proof, to demonstrate a novel site unequivocally by ligand binding, in our opinion, requires that a uniquely novel BSS be demonstrated. Some such evidence for ϵ sites that are selective for β-endorphin (35) and for λ sites that are selective for certain epoxymorphinans (36) has been adduced. With respect to other putative sites, such as μ_1 (33) or κ subtypes (37–40), the arguments rest primarily on poorly selective radioligands used with selective blockers of known sites. That approach leaves open the possibility of heterogeneous labeling due to radioligand binding at unknown and poorly blocked sites. We believe that site characterization should be based on ligands that are highly selective for the sites being characterized.

The theoretical value of gaining better understanding of the topography of related receptor types, as through LSP and BSS, is obvious. There are also practical values. Autoradiography or positron emission tomography scanning techniques for localizing specific receptor types place a premium on a very high degree of selectivity for the desired site, inasmuch as localized high densities of secondary sites may otherwise mislead. For these purposes, it would seem essential to determine LSP for each new candidate ligand. Furthermore, the therapeutic value of a new drug should be related to its selectivity for the receptor type or subtype that will be its therapeutic target. To develop useful new drugs that distinguish between closely related receptors, site-selective binding assays and quantitative measures of binding selectivity, such as described here, will be essential.

Acknowledgments

We thank the generous donors of ligands, whose names are listed in Experimental Procedures.

References

1. Ahlquist, R. P. A study of the adrenotropic receptors. *Am. J. Physiol.* **153**:586–600 (1948).
2. Leslie, F. M. Methods used for the study of opioid receptors. *Pharmacol. Rev.* **39**:197–249 (1987).
3. Lord, J. A., A. A. Waterfield, J. Hughes, and H. W. Kosterlitz. Endogenous opioid peptides: multiple agonists and receptors. *Nature (Lond.)* **267**:495–499 (1977).
4. James, I. F., C. Chavkin, and A. Goldstein. Preparation of brain membranes containing a single type of opioid receptor highly selective for dynorphin. *Proc. Natl. Acad. Sci. USA* **79**:7570–7574 (1982).
5. Chavkin, C., I. F. James, and A. Goldstein. Dynorphin is a specific endogenous ligand of the κ opioid receptor. *Science (Wash. D. C.)* **215**:413–415 (1982).
6. James, I. F., and A. Goldstein. Site-directed alkylation of multiple opioid receptors. I. Binding selectivity. *Mol. Pharmacol.* **25**:337–342 (1984).
7. Goldstein, A. Binding selectivity profiles for ligands of multiple receptor types: focus on opioid receptors. *Trends Pharmacol. Sci.* **8**:456–459 (1987).
8. Goldstein, A. Biology and chemistry of the dynorphin peptides, in *The Peptides* (J. Meienhofer and S. Udenfriend, eds.), Vol. 6. Academic Press, New York, 95–145 (1984).
9. Goldstein, A., J. J. Nestor, Jr., A. Naidu, and S. R. Newman. A multipurpose ligand with high affinity and selectivity for dynorphin (*kappa* opioid) binding sites. *Proc. Natl. Acad. Sci. USA* **85**:7375–7379 (1988).
10. Xu, H., J. Chen, and Z. Q. Chi. Ohmefentanyl: a new agonist for μ-opiate receptor. *Sci. Sin.* **28**:504–511 (1985).
11. Pelton, J. T., W. Kazmierski, K. Gulya, H. I. Yamamura, and V. J. Hruby. Design and synthesis of conformationally constrained somatostatin analogues with high potency and specificity for μ opioid receptors. *J. Med. Chem.* **29**:2370–2375 (1986).
12. Romer, D., H. H. Buscher, R. C. Hill, R. Maurer, T. J. Petcher, H. Zeugner, W. Benson, E. Finner, W. Milkowski, and P. W. Thies. Unexpected opioid activity in a known class of drug. *Life Sci.* **31**:1217–1220 (1982).
13. Gillan, M. G. C., and H. W. Kosterlitz. Spectrum of the *mu*-, *delta*- and *kappa*-binding sites in homogenates of rat brain. *Br. J. Pharmacol.* **77**:461–468 (1982).
14. Handa, B. K., A. C. Lane, J. A. H. Lord, B. A. Morgan, M. J. Rance, and C. F. C. Smith. Analogues of β-LPH$_{61-64}$ possessing selective agonist activity at μ-opiate receptors. *Eur. J. Pharmacol.* **70**:531–540 (1981).
15. Vonvoigtlander, P. F., and R. A. Lewis. Analgesic and mechanistic evaluation of spiradoline, a potent *kappa* opioid. *J. Pharmacol. Exp. Ther.* **246**:259–262 (1988).
16. Mosberg, H. I., J. R. Omnaas, and A. Goldstein. Structural requirements for δ opioid receptor binding. *Mol. Pharmacol.* **31**:599–602 (1987).
17. Roques, B. P., M. C. Fournie-Zaluski, G. Gacel, M. David, J. C. Meunier, B. Maigret, and J. L. Morgat. Rational design and biological properties of highly specific *mu* and *delta* opioid peptides. *Adv. Biochem. Psychopharmcol.* **33**:321–331 (1982).
18. Chang, K. J., E. T. Wei, A. Killian, and J. K. Chang. Potent morphiceptin analogs: structure-activity relationships and morphine-like activities. *J. Pharmacol. Exp. Ther.* **227**:403–408 (1983).
19. Vonvoigtlander, P. F., R. A. Lahti, and J. H. Ludens. U-50,488: a selective and structurally novel non-*mu* (*kappa*) opioid agonist. *J. Pharmacol. Exp. Ther.* **224**:7–12 (1983).
20. Mosberg, H. I., R. Hurst, V. J. Hruby, K. Gee, H. I. Yamamura, J. J. Galligan, and T. F. Burks. Bis-penicillamine enkephalins possess highly improved specificity toward *delta* opioid receptors. *Proc. Natl. Acad. Sci. USA* **80**:5871–5874 (1983).
21. Lahti, R. A., M. M. Mickelson, J. M. McCall, and P. F. Vonvoigtlander. [^{3}H] U-69593: a highly selective ligand for the opioid κ receptor. *Eur. J. Pharmacol.* **109**:281–284 (1985).
22. Munson, P. J., and D. Rodbard. LIGAND: a versatile computerized approach for characterization of ligand-binding systems. *Anal. Biochem.* **107**:220–239 (1980).
23. Goldstein, A., and R. W. Barrett. Ligand dissociation constants from competition binding assays: errors associated with ligand depletion. *Mol. Pharmacol.* **31**:603–609 (1987).
24. Cheng, Y. C., and Prusoff, W. H. Relationship between the inhibition constant (K_I) and the concentration of inhibitor which causes 50 per cent

inhibition (I_{50}) of an enzymatic reaction. *Biochem. Pharmacol.* **22**:3099–3102 (1973).
25. Pert, C. B., G. Pasternak, and S H. Snyder. Opiate agonists and antagonists discriminated by receptor binding in brain. *Science (Wash. D. C.)* **182**:1359–1361 (1973).
26. Simon, E. J., J. M. Hiller, J. Groth, and I. Edelman. Further properties of stereospecific opiate binding sites in rat brain: on the nature of the sodium effect. *J. Pharmacol. Exp. Ther.* **192**:531–537 (1975).
27. Paterson, S. J., L. E. Robson, and H. W. Kosterlitz. Control by cations of opioid binding in guinea pig brain membranes. *Proc. Natl. Acad. Sci. USA* **83**:6216–6220 (1986).
28. Shook, J. E., J. T. Pelton, P. K. Lemcke, F. Porreca, V. J. Hruby, and T. F. Burks. *Mu* opioid antagonist properties of a cyclic somatostatin octapeptide *in vivo*: identification of *mu* receptor-related functions. *J. Pharmacol. Exp. Ther.* **242**:1–7 (1987).
29. James, I. F., W. Fischli, and A. Goldstein. Opioid receptor selectivity of dynorphin gene products. *J. Pharmacol. Exp. Ther.* **228**:88–93 (1984).
30. Chavkin, C., and A. Goldstein. Specific receptor for the opioid peptide dynorphin: structure-activity relationships. *Proc. Natl. Acad. Sci. USA* **78**:6543–6547 (1981).
31. Borea, P. A., G. M. Bertelli, and G. Gilli. Temperature dependence of the binding of μ, δ and κ agonists to the opiate receptors in guinea-pig brain. *Eur. J. Pharmacol.* **146**:247–252 (1988).
32. Werling, L. L., P. S. Puttfarcken, and B. M. Cox. Multiple agonist-affinity states of opioid receptors: regulation of binding by guanyl nucleotides in guinea pig cortical, NG108-15, and 7315c cell membranes. *Mol. Pharmacol.* **33**:423–431 (1988).
33. Pasternak, G. W. Multiple *mu* opiate receptors: biochemical and pharmacological evidence for multiplicity. *Biochem. Pharmacol.* **35**:361–364 (1986).
34. Gairin, J. E., C. Gouarderes, H. Mazarguil, P. Alvinerie, and J. Cros. [D-Pro10]Dynorphin-(1–11) is a highly potent and selective ligand for *kappa* opioid receptors. *Eur. J. Pharmacol.* **106**:457–458 (1984).
35. Toogood, C. I. A., K. G. McFarthing, E. C. Hulme, and D. G. Smyth. Use of ^{125}I-Tyr^{27} β-endorphin for the study of β-endorphin binding sites in rat cortex. *Neuroendocrinology* **43**:629–634 (1986).
36. Grevel, J., V. Yu, and W. Sadee. Characterization of a labile naloxone binding site (*lambda* site) in rat brain. *J. Neurochem.* **44**:1647–1656 (1985).
37. Attali, B., C. Gouarderes, H. Mazarguil, Y. Audigier, and J. Cros. Evidence for multiple "*kappa*" binding sites by use of opioid peptides in the guinea-pig lumbo-sacral spinal cord. *Neuropeptides* **3**:53–64 (1982).
38. Nock, B., A. Rajpara, L. H. O'Connor, and T. J. Cicero. Autoradiography of [^{3}H]U-69593 binding sites in rat brain: evidence for κ opioid receptor subtypes. *Eur. J. Pharmacol.* **154**:27–34 (1988).
39. Zukin, R. S., M. Eghbali, D. Olive, E. M. Unterwald, and A. Tempel. Characterization and visualization of rat and guinea pig brain κ opioid receptors: evidence for κ_1 and κ_2 opioid receptors. *Proc. Natl. Acad. Sci. USA* **85**:4061–4065 (1988).
40. Clark, C. R., B. Birchmore, N. A. Sharif, J. C. Hunter, R. G. Hill, and J. Hughes. PD117302: a selective agonist for the κ-opioid receptor. *Br. J. Pharmacol.* **93**:618–626 (1988).